Analyst

PAPER

View Article Online
View Journal

Cite this: DOI: 10.1039/d0an01224f

A simple enzyme-catalyzed reaction induced "switch" type fluorescence biosensor based on carbon nitride nanosheets for the assay of alkaline phosphatase activity

Xi Zhu,[a,b] Huifeng Xu, *[c] Yan Zhan,[a] Wenjing Li,[a] Yongqiang Dong, [d] Lishuang Yu, [c] Yuwu Chi *[d] and Hongzhi Ye[c]

Received 18th June 2020,
Accepted 19th August 2020

DOI: 10.1039/d0an01224f

rsc.li/analyst

An enzyme-catalyzed fluorescence "switch" type sensor was constructed for the determination of alkaline phosphatase (ALP) activity by combining the fluorescence quenching effect of Ag^+ on ultrathin g-C_3N_4 nanosheets (CNNSs) with the simple redox reaction of AA and Ag^+. Briefly, Ag^+ exhibits a significant quenching effect on the fluorescence of CNNSs. Thus the fluorescence signal of the CNNS-Ag^+ system is extremely weak even in the presence of L-ascorbic acid-2-phosphate (AAP) ("off" state). When ALP coexists in the system, the enzyme can specifically catalyze the hydrolysis of AAP to form ascorbic acid (AA), which reduces Ag^+ to Ag^0. In this case, the fluorescence signal of the system is recovered ("on" state). Based on this principle, a signal-enhanced CNNS fluorescence sensor was developed to determine the activity of alkaline phosphatase. The experimental results show that the detection range of alkaline phosphatase is 0.5–20 U L^{-1}, and the detection limit is 0.05 U L^{-1} (S/N = 3). Meanwhile, this method was used to assay ALP in serum samples.

Introduction

Alkaline phosphatase (ALP) is a common and important membrane-bound protease in the human body and widely distributed in tissues such as the liver, bone, intestine, kidneys and placenta. ALP has a broad substrate specificity and is capable of catalyzing the dephosphorylation of small molecules, nucleic acids and proteins.[1] The catalytic reaction of ALP can repair the phosphate group to a hydroxyl group at the end of DNA. Therefore, it plays an important role in many biological processes, including gene transduction, cell metabolism and neuronal action. Meanwhile, some human orthopaedic diseases[2] (osteoblastoma, malformation osteitis and rickets), liver diseases[3] (hepatitis and obstructive jaundice), prostate cancer and diabetes[4,5] are all closely related to the level of ALP in the human body. In view of the important role of ALP, the construction of highly sensitive and selective ALP detection methods is of great value.

To date, many efforts are dedicated to fast, efficient, and easy-to-handle analytical methods, such as fluorescence,[6–9] chemiluminescence,[10] bioluminescence,[11] colorimetric,[12–14] electrochemical,[15–17] and surface-enhanced Raman spectroscopy.[18,19] Among them, fluorescent spectrometry not only offers favourable analytical performance with high sensitivity with simple instruments and operation, but is also flexible to combine with a microscope to achieve direct dynamic analysis in a single cell. In recent years, organic dyes[9,20] and nanodots[13,21] as probes have been applied in ALP sensing. Although these proposed methods provide different perspectives for analyzing ALP, they suffer from several disadvantages, including poor photostability, complex preparation, and high costs. The development of analytical methods with simple operation, low sample consumption and low costs for ALP activity is still a challenging task.

Recently, g-C_3N_4 nanosheets (CNNSs), a two-dimensional (2D) semiconductor nanomaterial, not only have excellent fluorescence characteristics and dispersibility, but also have many advantages such as easy synthesis, low costs, non-toxicity and good biocompatibility. In this work, a simple strategy was constructed for monitoring ALP activity by the fluorescence

[a]College of Life Sciences, Fujian Provincial Key Laboratory of Agroecological Processing and Safety Monitoring, Fujian Agriculture and Forestry University, Fuzhou, Fujian, 350002, China
[b]College of Biological, Chemical Sciences and Engineering, Jiaxing University, Jiaxing 314001, PR China
[c]Fujian Key Laboratory of Integrative Medicine on Geriatrics, Academy of Integrative Medicine, Fujian University of Traditional Chinese Medicine, Fuzhou, Fujian, P. R. China. E-mail: xuhf@fjtcm.edu.cn
[d]MOE Key Laboratory of Analysis and Detection for Food Safety, State Key Laboratory of Photo Catalysis on Energy and Environment, and College of Chemistry, Fuzhou University, Fujian 350108, China. E-mail: y.w.chi@fzu.edu.cn; Fax: +86-591-22866137; Tel: +86-591-22866137

annihilation effect of Ag^+ toward CNNSs and the specific catalytic hydrolysis ability of ALP to the substrate L-ascorbic acid 2-phosphate (AAP). The principle is simply described as follows: ALP can catalyze the dephosphorylation of its substrate AAP into L-ascorbic acid (AA). Then AA will reduce Ag^+ to Ag^0, inhibiting the fluorescence quenching ability of Ag^+ to CNNSs. This sensor can monitor the activity of ALP with high sensitivity and exhibits several advantages, including easy operation, low costs, and good selectivity.

Experimental section

Chemical reagents and apparatus

Dicyanodiamide and silver nitrate ($AgNO_3$, 99.9995%) were purchased from Sigma. L-Ascorbic acid (AA) and L-ascorbic acid 2-phosphate (AAP) were purchased from Fuchen Chemical Reagent Co., Ltd (Tianjin, China). Alkaline phosphatase (ALP), bovine albumin (BSA, >98.0%), glucose oxidase, lysozyme, *etc*. were purchased from Sangon Biotech (Shanghai) Co., Ltd. The experimental water was ultrapure water obtained from a Millipore Milli-Q system (resistance was 18.2 MΩ). The buffer solution was 20 mM Tris-acetic acid (TAE) with pH 9.0.

Fluorescence spectra were recorded on a fluorescence spectrophotometer (Cary Eclipse, Varian). Transmission electron microscopy (TEM) was performed on an electronic microscope (TecnaiG2 F20S-TWIN 200 kV). UV-vis absorption spectra were recorded with a UV 1800 spectrometer.

Preparation of CNNSs

The CNNSs were prepared according to the previously reported literature.[22] Firstly, 3 g of dicyanamide was heated at 600 °C in a tube furnace for 2 h under air conditions with a ramp of about 3 °C min^{-1} for the heating processes to gain pale yellow bulk g-C_3N_4. Next, 100 mg of bulk g-C_3N_4 powder was ground well with a mortar and a pestle, followed by dispersion in 100 mL of water and ultrasound treatment for 16 h. After centrifugation at about 6000 rpm, the supernatant was collected and concentrated on a rotary evaporator under reduced pressure. A milk-like CNNS suspension was obtained after the above preparation procedure. The mass concentration of the CNNS suspension was calculated by weighing the power dried from a certain volume of the suspension. The final concentration of CNNSs used in the experiment was 0.06 mg mL^{-1}.

Detection of AA

AA of different concentrations was added to the TAE solution (20 mM, pH 9.0) containing 60 μM Ag^+, and then incubated at 37 °C for 30 min. Subsequently, CNNSs were added to the solution and mixed thoroughly before fluorescence detection.

Detection of ALP

Alkaline phosphatase of different activities was added to the TAE solution (20 mM, pH 9.0) containing 600 μM AAP and 60 μM Ag^+, and then incubated at 37 °C for a period of time. Subsequently, CNNSs were added to the mixture for 2 min before fluorescence detection.

Determination of serum samples

The serum samples used in the experiment were provided by Fuzhou Second People's Hospital. After the serum samples were diluted 10 times, 50 μL of serum was added to TAE solution (20 mM, pH 9.0) containing 600 μM AAP and 60 μM Ag^+. After shaking at 37 °C for 4 h, 0.06 mg mL^{-1} CNNS was thoroughly mixed for 2 min before detection.

Results and discussion

Characterization of CNNSs

In the TEM image (Fig. 1A), the as-prepared CNNSs show lamellar and planar thin nanosheets. The zeta potential of CNNSs (displayed in the inset of Fig. 1A) was −23.5 mV in deionized water, indicating that the surface of CNNSs was negatively charged, so they can be well dispersed in water for a long time without aggregation. The optical properties of CNNSs were also investigated. Under a 365 nm UV light lamp, the homogeneous CNNS solution exhibits bright blue fluorescence (the inset in Fig. 1B). Further, CNNSs possess the maximum emission peak at about 440 nm upon an excitation wavelength of 330 nm (Fig. 1B). The XRD characterization of CNNSs is shown in Fig. 1C. The peak of (002) at 27.6° is attributed to the stacking of the aromatic segments in the g-C_3N_4 graphitic-like structure.[23,24] The low-angle diffraction at 13.3° is indexed to the (100) plane of CNNSs.[24] The feeble intensity of this peak indicated the successful preparation of CNNSs. Atomic force

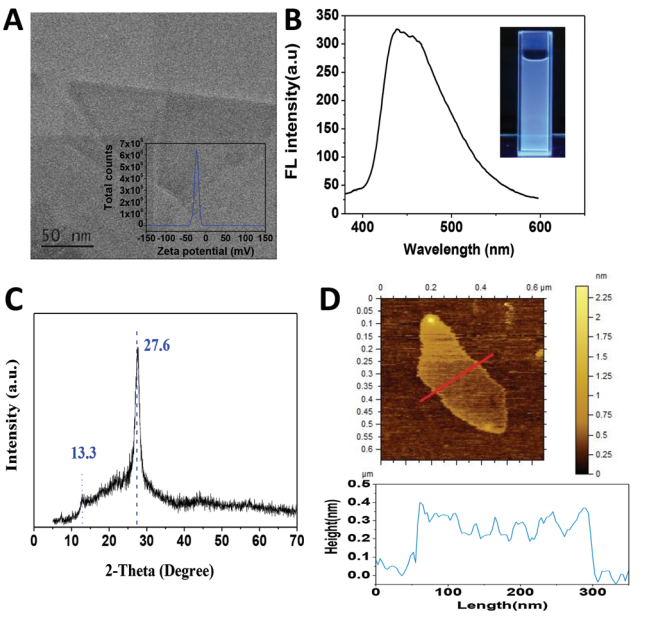

Fig. 1 (A) TEM image, inset: zeta potential of CNNSs, and (B) fluorescence spectrum of CNNSs. Inset: The photograph of CNNSs under UV light. (C) XRD patterns and (D) AFM of CNNSs.

microscopy (AFM) images in Fig. 1D clearly show that CNNSs used herein are ultrathin nanosheets with a thickness of about 0.4 nm, which also provides evidence of successful preparation of ultrathin CNNSs.

Sensing principle

The detection principle of this work is illustrated in Scheme 1. When Ag^+ and AAP coexisted in the solution, no reaction occurred, and in this case, the fluorescence of CNNSs was significantly quenched by Ag^+ after it was introduced into the solution. In this state, this fluorescence response of the system was called the "OFF" state. Next, the presence of ALP will hydrolyse its substrate AAP to AA, which can further reduce Ag^+ to Ag^0 and weaken the quenching effect of Ag^+ toward CNNSs. The fluorescence signal of the system recovered under this circumstance, called the "ON" state. Based on the change of the fluorescence intensity, therefore, this detection method can be used to monitor the activity of ALP.

Feasibility analysis

In order to confirm the feasibility of the method, the following verification experiments were carried out. Firstly, the effects of Ag^+, AA and AAP on the fluorescence of CNNSs were investigated (Fig. 2A). The fluorescence intensity of CNNSs stayed unchanged in the presence of AA and AAP, indicating that AA and AAP have no significant effect on the fluorescence of CNNSs. However, the fluorescence signal of CNNSs significantly decreased in the presence of Ag^+ owing to the obvious quenching effect of Ag^+. Moreover, when AAP and Ag^+ coexisted, the fluorescence signal of the solution was similar to that of the solution with only Ag^+. This is due to the inability of AAP to react with Ag^+. By contrast, the fluorescence intensity obviously enhanced in the presence of AA and Ag^+. This revealed that the presence of AA can significantly suppress the quenching effect of Ag^+ to CNNSs by reducing Ag^+ to elemental Ag^0, resulting in the fluorescence recovery.

Next, the influence of ALP on the fluorescence of the Ag^+-CNNS system with/without AAP was further verified. As shown in Fig. 2B, it was confirmed that ALP has negligible influence on the fluorescence of CNNSs beforehand. Then, the fluorescence signal of the Ag^+-CNNS system was very weak in the presence of AAP. Similarly, without AAP, the solution still exhibited weak fluorescence in the presence of ALP, showing that there was no reaction between ALP and the Ag^+-CNNS system. However, when AAP and ALP coexisted in the Ag^+-CNNS system, the fluorescence was remarkably enhanced. This can be attributed to the catalytic hydrolysis of AAP by ALP to form AA, followed by the reduction of Ag^+ by AA, inhibiting the quenching effect of Ag^+ toward the fluorescence of CNNSs.

Additionally, since it has been reported that AgNPs also have a serious quenching effect on the fluorescence of CNNSs,[25] it is necessary to check out whether AgNPs could be formed in this experimental system. UV-Vis absorption spectra were recorded to get insight into the difference between AgNPs and the product of AA reaction with Ag^+, and fluorescence spectra were also recorded to check out the influence of AgNPs on CNNSs. Fig. 2C provides the absorption spectra of AgNPs synthesized according to a previous report[26] using AA as the reduction agent for comparison with the product in the present system. It is shown that no visible absorption peak could be observed for the solution containing AA and Ag^+, while the AgNP solution exhibited an obvious absorption at *ca.* 410 nm. It can be deduced that AgNPs cannot be formed by reducing Ag^+ with AA under the proposed experimental conditions. As shown in Fig. 2D, the fluorescence intensity of CNNSs in the presence of AgNPs showed striking suppression compared with that of CNNSs only, indicating that AgNPs indeed have an intense quenching effect on CNNSs, which is

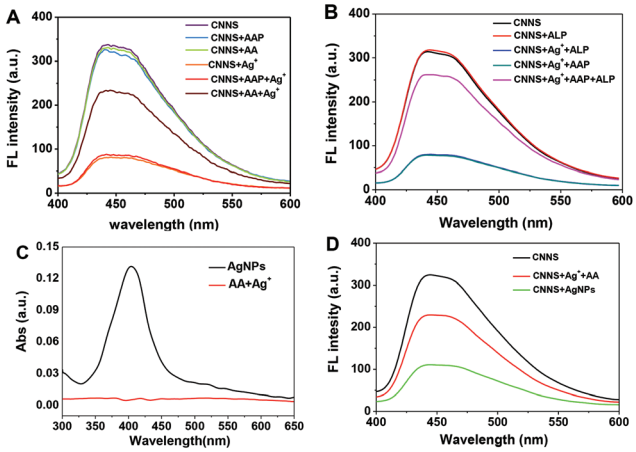

Fig. 2 (A) Fluorescence spectra of CNNSs in TAE buffer solution (20 mM, pH 9.0) containing different substances. The concentrations of Ag^+, AA and AAP were 60 μM, 300 μM, and 600 μM, respectively. (B) Fluorescence spectra of Ag^+-CNNS in the presence of different conditions in TAE buffer solution (20 mM, pH 9.0). The concentrations of Ag^+ and AAP were 60 μM and 600 μM, respectively. The activity of ALP was 12 U L^{-1}. (C) UV-vis spectra of AgNPs and the product of AA reaction with Ag^+ in TAE buffer solution (20 mM, pH 9.0) and (D) fluorescence spectra of CNNSs in the presence of AgNPs (60 μM) and the product of AA reaction with Ag^+ in TAE buffer solution (20 mM, pH 9.0). The concentrations of Ag^+ and AA were 60 μM and 300 μM, respectively.

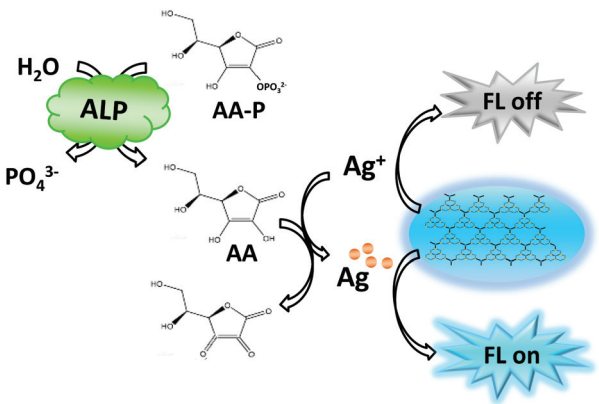

Scheme 1 Schematic representation of the sensing principle for ALP activity.

consistent with the previous report.[25] Under the same circumstances, the fluorescence of CNNSs exhibited a much stronger signal in the reaction solution of AA and Ag^+ than in the solution of AgNPs, inferring the essential difference between AgNPs and the product of AA and Ag^+ in this detection system.

Overall, from the above series of experiments, it can be verified that this method using the AAP-Ag^+-CNNS system to detect ALP activity is feasible.

Optimization of experimental conditions

Considering that several metal ions are reported to be capable of quenching the fluorescence of graphitic carbon nitride,[24,27–29] the changes of CNNS fluorescence were investigated in the absence and presence of AA with these main metal ions, respectively. Fig. 3 shows the fluorescence intensities with different metal ions and AA, where F_0 and F_1 represent the fluorescence signals of CNNSs with different metal ions in the absence and presence of AA, respectively. It is observed that the fluorescence of CNNSs is significantly quenched by Ag^+ without AA compared with other metals except Cu^{2+}. Cu^{2+} also showed a quenching effect on CNNSs, which is consistent with previous reports[24,29] despite its weaker influence than Ag^+. However, in the presence of AA, the fluorescence intensity of Cu^{2+}-CNNS failed to recover as that of Ag^+-CNNS. The reason may be due to the fact that the redox potential of Ag^+ transferred to the elemental state is much higher than that of Cu^{2+} (the reduction potential value $E^{\circ}_{(Ag^+/Ag^0)}$ was +0.7996 V and $E^{\circ}_{(Cu^{2+}/Cu^0)}$ was +0.159 V *vs.* NHE in aqueous solution at 25 °C, respectively[30]). It can be deducted that Ag^+ is easier to reduce by AA under the same conditions. Furthermore, compared with Ag^+, Cu^{2+} needs to consume twice the amount of AA to generate Cu^0. Based on the above results, Ag^+ was used as the quenching source of CNNSs in this work.

The amount of Ag^+ and the reaction time between Ag^+ and CNNSs were examined subsequently. From Fig. 4A, it is observed that the fluorescence of CNNSs decreased linearly with the addition of Ag^+ and reached a stable value when the concentration of Ag^+ was 60 μM. Thereafter, the addition of Ag^+ does not decrease the fluorescence intensity again. So the concentration of Ag^+ was set at 60 μM in the subsequent

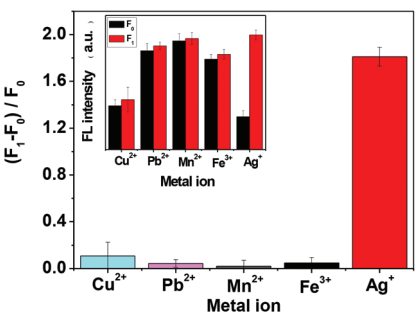

Fig. 3 Relative change of the fluorescence intensity of CNNSs in the presence of different metal ions (60 μM) and 100 μM AA. Inset: The fluorescence intensity before (F_0) and after (F_1) adding metal ions. Buffer solution: TAE buffer solution (20 mM, pH 9.0).

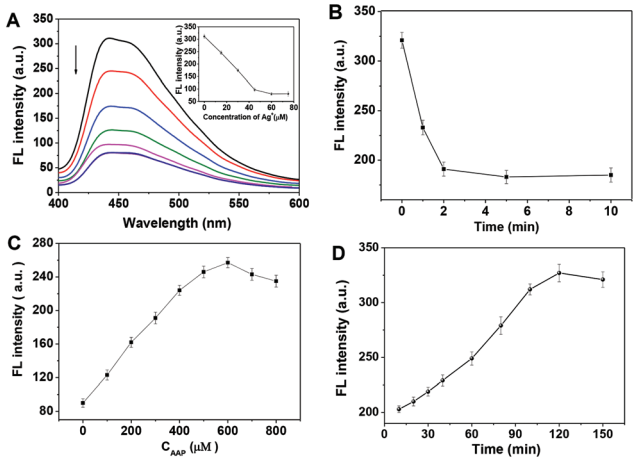

Fig. 4 (A) The fluorescence spectra of CNNSs under different concentrations of Ag^+. Inset: The fluorescence intensity of CNNSs under different Ag^+ concentrations. (B) The reaction time of Ag^+ and CNNSs. (C) Fluorescence intensities under different concentrations of AAP and (D) fluorescence intensities under different reaction times of AAP (600 μM) with ALP (12 U L^{-1}).

experiments. As elucidated in previous reports,[31–33] the quenching mechanism of Ag^+ towards CNNSs could be attributed to the strong absorption ability of Ag^+ with the cyano group on the CNNS surface,[31] as well as the appropriate redox potential of Ag^+ lying between the CB and VB of CNNSs, which makes photoinduced electron transfer (PET) effect liable to occur and eventually leads to a significant fluorescence quenching phenomenon.[32,33]

The reaction time of Ag^+ and CNNSs is further investigated. As shown in Fig. 4B, the fluorescence of CNNSs was dramatically quenched within 2 min after adding Ag^+ in the solution, and reached a plateau in 5 min. It is apparent that the interaction of Ag^+ with CNNSs is quite fast. In addition, it was also found that the reaction process of Cu^{2+} and CNNSs was much more gradual and required about 10 min to reach quenching saturation. These observations agree with previous reports that the adsorption energy barriers in the Ag^+-g-C_3N_4 system are smaller than those of the Cu^{2+}-g-C_3N_4 system;[24,33] that is, Ag^+ binds to CNNSs much more rapidly than Cu^{2+} and leads to a faster response of fluorescence changes. Thus, in order to reduce the possible interference of Cu^{2+}, the reaction time of Ag^+ and CNNSs is chosen as 2 min.

The influences of AAP concentration and the reaction time of AAP with ALP were then investigated. The fluorescence intensity of the system gradually increased with the increase of AAP concentration and reached the maximum value when the AAP concentration was 600 μM (Fig. 4C). Overload of the substrate may inhibit the enzyme activity; thus, the concentration of the substrate AAP was set at 600 μM. As shown in Fig. 4D, the fluorescence of Ag^+-CNNS reaches a plateau when the reaction time of AAP with ALP lasts for 120 min. Thus, the reaction time was set at 120 min in the following experiments.

Once the main experimental conditions were determined, we next investigated the relationship between the fluorescence

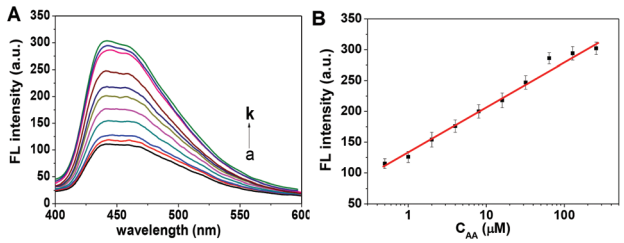

Fig. 5 (A) Fluorescence spectra of the Ag^+-CNNS system with different concentrations of AA in TAE buffer solution (20 mM, pH 9.0) and (B) plot of the fluorescence intensity against the logarithm of AA concentration. Curves a to k represent the concentrations of 0, 0.5, 1, 2, 4, 8, 16, 32, 64, 128 and 256 μM, respectively. [Ag^+] = 60 μM.

intensity of Ag^+-CNNS and the concentrations of AA. The results in Fig. 5 showed that the fluorescence intensity of the Ag^+-CNNS system increased with the addition of AA concentration, which indicates that the increase of AA concentration promotes the reaction process between AA and Ag^+, leading to gradual recovery of the fluorescence signal. A linear relationship between the fluorescence intensity and the logarithm of the concentration of AA in the range of 0.5–256 μM was also oversized.

ALP detection

Under the optimal conditions, the relationship between the fluorescence intensity and ALP activities was further investigated. It can be seen from Fig. 6A that as the ALP activity increases, the fluorescence of the system increases, indicating that AA was gradually produced in the solution due to ALP-catalyzed hydrolysis of the substrate AAP. Then AA further reduces Ag^+ to the silver element, thereby weakening the quenching effect of Ag^+ on the CNNS fluorescence, resulting in the recovery of the fluorescence signal. There is a certain linear relationship between the fluorescence intensity and the logarithm of the activity of ALP in the range of 0.5–20 U L^{-1}. As shown in Fig. 6B, the linear equation is as follows:

$$Y = 64.10X + 191.88 \ (R^2 = 0.997)$$

where Y represents the fluorescence intensity and X represents the activity of ALP. The limit of detection (LOD) was calculated

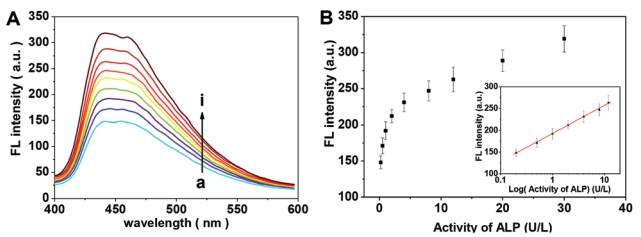

Fig. 6 (A) The fluorescence spectra under different activities of ALP; curves a to i represent the activity of 0, 0.5, 1, 2, 4, 8, 12, 20, and 30 U L^{-1}, respectively. (B) The fluorescence intensity as a function of [ALP]; inset: the linearity of FL intensity with respect to logarithmic [ALP]. Buffer solution: TAE buffer solution (20 mM, pH 9.0) with 60 μM Ag^+ and 600 μM AAP.

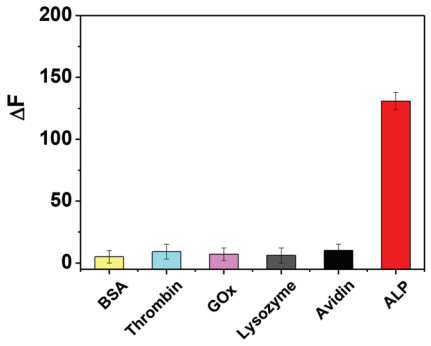

Fig. 7 The selectivity of the proposed method for ALP. Buffer solution: TAE buffer solution (20 mM, pH 9.0) with 60 μM Ag^+ and 600 μM AAP. The concentrations of the interferents were 1 mM, and the activity of ALP was 1 U L^{-1}.

to be 0.05 U L^{-1} based on signal/noise = 3, which is more sensitive than that of the previous methods.[34–38]

Selective investigation

Several proteins such as bovine serum albumin (BSA), thrombin, glucose oxidase (GOx), lysozyme and avidin were selected as interference proteins to evaluate the selectivity of the sensor. Fig. 7 shows the fluorescence changes ΔF with different proteins. The fluorescence change ΔF is defined as $F_t - F_0$, where F_t and F_0 stand for the fluorescence response with and without these proteins. It is obvious that there are weak fluorescence changes in the absence of other interference proteins, while only the target molecule ALP can induce the enhancement of the fluorescence change. However, it has to be pointed out that, if the detection sample contains high concentrations of copper ions, halide ions or small molecules like cysteine which can strongly bind with Ag^+, pretreatment is required to remove or mask them to avoid negative influence on the final result.

The reproducibility of this method was also tested by performing five successive assays for the detection of ALP (2 U L^{-1}). The RSD was calculated to be 3.7%, indicating the good reproducibility of the proposed method.

Detection of serum samples

In order to examine the utility of the method, it was applied to assay ALP in serum samples. Here, six different serum samples were selected, and each was measured three times in parallel. The results of the measurement are shown in Table 1.

Table 1 The determination of ALP in serum samples

No.	This method (U L^{-1})	Rate method (U L^{-1})
1	90.4 ± 2.5	92.6
2	126.9 ± 4.5	130.1
3	147.9 ± 6.5	145.0
4	98.8 ± 4.8	100.2
5	153.9 ± 5.5	150.6
6	87.6 ± 6.3	86.6

The ALP activities in the serum samples ranged from 87.6 U L^{-1} to 153.9 U L^{-1}. The results were basically consistent with those of the standard method (rate method).

Conclusions

Combining the fluorescence quenching effect of Ag^{+} on CNNSs with enzyme-induced substrate hydrolysis, a simple fluorescence method was established for the detection of ALP. Compared with traditional analytical methods for ALP, this method does not require radioisotopes, and is easy to operate. Moreover, this method was used to assay ALP in the serum, indicating that CNNSs as a promising material can be used for early diagnosis of some diseases.

Conflicts of interest

There are no conflicts to declare.

Acknowledgements

This project was financially supported by NSFC (81773894), the Natural Science Foundation of Fujian Province, China (2018J01871, 2019Y4009, and 2017Y0047), and Open Project of Jiaxing University Key Laboratory of Rapid Detection Technology and Instruments for Environment and Food. X. Zhu thanks the University Distinguished Young Research Talent Training Program of Fujian Province, and H. Xu also thanks the Natural Science Funds of Fujian Province for Distinguished Young Scholar (2019J06021).

References

1 J. E. Coleman, *Annu. Rev. Biophys. Biomol. Struct.*, 1992, **21**, 441–483.
2 M. M. Couttenye, P. C. D'Haese, V. O. Van Hoof, E. Lemoniatou, W. Goodman, G. A. Verpooten and M. E. De Broe, *Nephrol., Dial., Transplant.*, 1996, **11**, 1065–1072.
3 P. Colombatto, A. Randone, G. Civitico, G. J. Monti, L. Dolci, N. Medaina, F. Oliveri, G. Verme, G. Marchiaro and R. Pagni, *J. Viral Hepatitis*, 1996, **3**, 301–306.
4 J. A. Lorente, H. Valenzuela, J. Morote and A. Gelabert, *Eur. J. Nucl. Med. Mol. Imaging*, 1999, **26**, 625–632.
5 N. J. Fernandez and B. A. Kidney, *Vet. Clin. Pathol.*, 2007, **36**, 223–233.
6 G. Li, H. Fu, X. Chen, P. Gong, G. Chen, L. Xia, H. Wang, J. You and Y. Wu, *Anal. Chem.*, 2016, **88**, 2720–2726.
7 W. Kang, Y. Ding, H. Zhou, Q. Liao, X. Yang, Y. Yang, J. Jiang and M. Yang, *Microchim. Acta*, 2014, **182**, 1161–1167.
8 Y. Hu, Y. He, Y. Han, Y. Ge, G. Song and J. Zhou, *Microchim. Acta*, 2018, **186**, 5–11.
9 L. Xu, X. He, P. Ma, X. Liu, F. Zhang, Y. Sun, D. Song and X. Wang, *Dyes Pigm.*, 2018, **159**, 584–589.
10 V. F. Ximenes, A. Campa, W. J. Baader and L. H. Catalani, *Anal. Chim. Acta*, 1999, **402**, 99–104.
11 W. Zhou, C. Andrews, J. Liu, J. W. Shultz, M. P. Valley, J. J. Cali, E. M. Hawkins, D. H. Klaubert, R. F. Bulleit and K. V. Wood, *ChemBioChem*, 2008, **9**, 714–718.
12 H. Wei, C. Chen, B. Han and E. Wang, *Anal. Chem.*, 2008, **80**, 7051–7055.
13 J. Wang, P. Ni, C. Chen, Y. Jiang, C. Zhang, B. Wang, B. Cao and Y. Lu, *Microchim. Acta*, 2020, **187**, 115–122.
14 T. Wu, W. Hou, Z. Ma, M. Liu, X. Liu, Y. Zhang and S. Yao, *Microchim. Acta*, 2019, **186**, 123–129.
15 C. Shen, X. Li, A. Rasooly, L. Guo, K. Zhang and M. Yang, *Biosens. Bioelectron.*, 2016, **85**, 220–225.
16 B. Kazakevičienė, G. Valinčius, M. Kažemėkaitė and V. Razumas, *Electroanalysis*, 2008, **20**, 2235–2240.
17 L. Sappia, B. Felice, M. A. Sanchez, M. Martí, R. Madrid and M. I. Pividori, *Sens. Actuators, B*, 2019, **281**, 221–228.
18 C. Ruan, W. Wang and B. Gu, *Anal. Chem.*, 2006, **78**, 3379–3384.
19 D. Sun, F. Cao, L. Cong, W. Xu, Q. Chen, W. Shi and S. Xu, *Lab Chip*, 2019, **19**, 335–342.
20 J. Sun, J. Zhao, X. Bao, Q. Wang and X. Yang, *Anal. Chem.*, 2018, **90**, 6339–6345.
21 F. Niu, Y.-L. Ying, X. Hua, Y. Niu, Y. Xu and Y.-T. Long, *Carbon*, 2018, **127**, 340–348.
22 H. Xu, X. Zhu, Y. Dong, H. Wu, Y. Chen and Y. Chi, *Sens. Actuators, B*, 2016, **236**, 8–15.
23 Y. Zhang, Q. Pan, G. Chai, M. Liang, G. Dong, Q. Zhang and J. Qiu, *Sci. Rep.*, 2013, **3**, 1943.
24 H. Huang, R. Chen, J. Ma, L. Yan, Y. Zhao, Y. Wang, W. Zhang, J. Fan and X. Chen, *Chem. Commun.*, 2014, **50**, 15415–15418.
25 Y. Li, M. Wan, G. Yan, P. Qiu and X. Wang, *J. Pharm. Anal.*, 2020, DOI: 10.1016/j.jpha.2020.04.007.
26 H. Li, H. Xia, W. Ding, Y. Li, Q. Shi, D. Wang and X. Tao, *Langmuir*, 2014, **30**, 2498–2504.
27 J. Tian, Q. Liu, A. M. Asiri, A. O. Al-Youbi and X. Sun, *Anal. Chem.*, 2013, **85**, 5595–5599.
28 S. Zhang, J. Li, M. Zeng, J. Xu, X. Wang and W. Hu, *Nanoscale*, 2014, **6**, 4157–4162.
29 N. Cheng, P. Jiang, Q. Liu, J. Tian, A. M. Asiri and X. Sun, *Analyst*, 2014, **139**, 5065–5068.
30 A. Bard, *Standard potentials in aqueous solution*, Routledge, 2017.
31 Q. Zhang, Y. Chai, M. Cao, F. Yang, L. Zhang and W.-L. Dai, *Appl. Surf. Sci.*, 2020, **503**, 143891.
32 W. Bian, H. Zhang, Q. Yu, M. Shi, S. Shuang, Z. Cai and M. M. Choi, *Spectrochim. Acta, Part A*, 2016, **169**, 122–127.
33 S. Cao, H. Chen, F. Jiang, Z. Hu and X. Wang, *ACS Appl. Mater. Interfaces*, 2018, **10**, 44624–44633.
34 X. Zhao, Y. Liu and K. S. Schanze, *Chem. Commun.*, 2007, 2914–2916, DOI: 10.1039/b706629e.
35 Y. Liu and K. S. Schanze, *Anal. Chem.*, 2008, **80**, 8605–8612.
36 H. Jiang and X. Wang, *Anal. Chem.*, 2012, **84**, 6986–6993.
37 H. Wang, L. Mu, G. She, H. Xu and W. Shi, *Sens. Actuators, B*, 2014, **203**, 774–781.
38 L. Zhang, J. Zhao, M. Duan, H. Zhang, J. Jiang and R. Yu, *Anal. Chem.*, 2013, **85**, 3797–3801.

